High Pressure Research, 1997, Vol. 15, pp. 201-220
Reprints available directly from the publisher
Photocopying permitted by license only

PHASE TRANSFORMATIONS OF AMORPHOUS GaSb-Ge ALLOY AT HIGH PRESSURES

V. E. ANTONOV, O. I. BARKALOV, E. G. PONYATOVSKY* and S. A. ZAVOLOVICH

Institute of Solid State Physics, Russian Academy of Sciences 142432, Chernogolovka, Moscow District, Russia

(Received May 15, 1996; in final form June 10, 1996)

Phase transformations occuring in the initially amorphous bulk $(GaSb)_{38}Ge_{24}$ semiconductor at pressures to 7.7 GPa and temperatures to 330°C were studied using the measurement of the electrical resistance supplemented by the X-ray examination of the samples quenched to 100 K after a high pressure treatment. The obtained experimental data and model calculations were then used to construct the *T–P* diagram of metastable equilibria between the crystalline metallic high-pressure phase (*hpp*) and two unordered phases, semiconducting (*sup*) and metallic (*mup*), which are either amorphous or liquid depending on the temperature. The line of the $hpp \rightleftarrows mup$ equilibrium (the melting curve of the high-pressure phase) was shown to terminate at a critical point where the *mup* becomes thermodynamically unstable as a phase. The line of the $hpp \rightleftarrows sup$ equilibrium conditions the effect of solid state amorphization of the high-pressure phase at decreasing pressure.

KEY WORDS: Solid state amorphization, high pressures.

1. INTRODUCTION

One of the most interesting and thoroughly studied effects of pressure on amorphous materials is the discontinues transition of the semiconducting amorphous substances to a metallic state. The transition was observed at room temperature in a number of different substances and was either irreversible (in amorphous Ge[1], Se[2], InSb[3], etc.) or reversible (in amorphous Si[1], $Se_{80}Te_{20}$[2], $(GaSb)_{36.5}Ge_{27}$[4], etc.). The high-pressure metallic state of all studied samples was crystalline.

The present paper reports on the phase transformations occurring in the initially amorphous $(GaSb)_{38}Ge_{24}$ alloy at temperatures from 17 to 330°C and pressures to 7.7 GPa. The studied *T–P* region involves the regions of reversible and irreversible crystallization and phase transitions between the thermodynamically equilibrium crystalline low-pressure and high-pressure phases. This allows the understanding of interrelations of the metastable and stable equilibria in the system.

The starting amorphous $(GaSb)_{38}Ge_{24}$ alloy was produced by the method[5] of spontaneous amorphization of a quenched high-pressure phase in the course of its heating at ambient pressure. The advantage of this method is the possibility to

---

*Author for Correspondence.

obtain bulk homogeneous amorphous samples. The method was earlier successfully applied to produce amorphous semiconductors GaSb, Cd–Sb, Zn–Sb and Al–Ge[6]. The GaSb–Ge alloy was chosen for the present investigation at elevated temperatures because its amorphous state should have higher thermal stability according to Ref. 7 where the amorphous samples were prepared by decompression of the high-pressure phase at room temperature.

2. SAMPLE PREPARATION AND EXPERIMENTAL DETAILS

To make the sample amorphous by using the method described in Ref. 5, one needs first transform it to a single-phase high-pressure state. In order to select the GaSb–Ge alloy with the maximum germanium content which forms this state at 7.5 GPa, we tried five GaSb–Ge alloys containing 12, 24, 30, 36 and 50 at.% Ge. Synthesis of the GaSb and Ge high-pressure phases requires about 6 and 9 GPa, respectively[8]. The pressure of 7.5 GPa was chosen because at $P \leqslant 7.5$ GPa our technique allowed synthesis of the GaSb–Ge pellets large enough to carry out all necessary measurements on the samples cut from one and the same pellet.

The alloys were prepared by alloying appropriate amounts of Ga, Sb and Ge (each 99.999 wt.% pure) in evacuated quartz tubes and subsequent quenching into a cold water bath. The obtained ingots were crushed into powder in an agate mortar, X-rayed at 100 K (Fig. 1) and pressed into pellets 8 mm in diameter and 5 mm thick. Each pellet was put in a Teflon container, the container was placed in a Toroid-type high-pressure chamber, exposed to 7.5 ± 0.5 GPa and 250 ± 7°C for 24 *h* and cooled

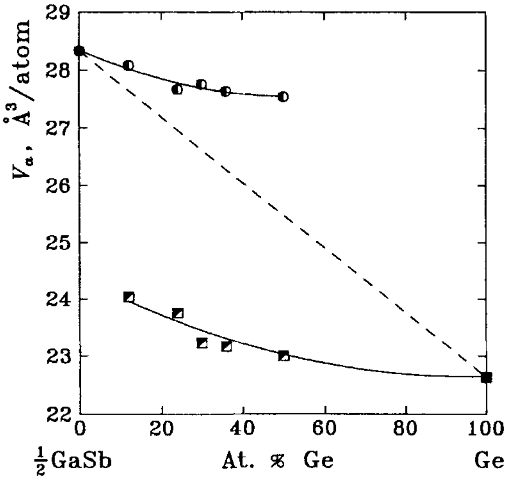

Figure 1 Volume V_a per atom of the cubic sphalerite-like (circles) and diamond-like (squares) phases of the GaSb–Ge alloys at ambient pressure and 100 K as a function of the average germanium content of the samples. The half-blackened symbols refer to the two-phase samples. The dashed line represents the linear dependence (the Vegard's rule) observed for the GaSb–Ge continuous solid solutions[10]. $V_a = a^3/8$, where a is the lattice parameter.

to 100 K together with the chamber. Then the pressure was lowered to the ambient one, the pellet was taken out of the chamber and X-rayed at 100 K (Fig. 2). The X-ray measurements in this work were carried out on a DRON–2.0 diffractometer using FeK$_\alpha$ radiation.

Stable and metastable equilibria in the crystalline quasi-binary GaSb–Ge alloys at ambient pressure are rather throughly studied. In the equilibrium phase diagram[9], there is a eutectic at 630°C, 40 at.% Ge with the maximum solid solubility of 2 at.% Ge in GaSb (sphalerite-like structure) and 8 at.% GaSb in Ge (diamond-like structure). Rapid quenching from the melt[10] allows obtaining metastable continuous solid solutions GaSb–Ge. The sphalerite-like structure of the solutions depleted of Ge transforms to the disordered diamond-like structure at approximately 40 at.% Ge. The concentration dependence of the atomic volume, V_a, of the solutions well obeys the Vegard's rule (dashed line in Fig. 1).

As is seen from Figure 1, the starting GaSb–Ge alloys prepared in the present work were two-phase in agreement with the equilibrium phase diagram[9]. The atomic volumes and, therefore, the compositions of the sphalerite-like and diamond-like phases varied, however, with the average composition of the alloy. These compositions thus were apparently non-equilibrium. From the comparison of the observed V_a values with the dependence for the continuous GaSb–Ge solid solutions shown by the dashed line, one could gather, in particular, that the diamond-like phases of the samples with 36 and 50 at.% Ge contain about 90 and 93 at.% Ge, respectively.

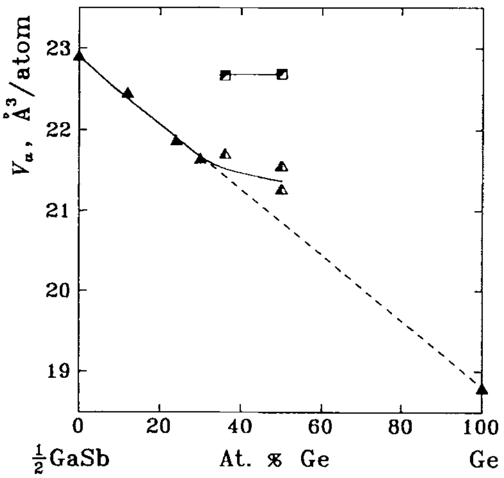

Figure 2 Volume V_a per atom of the tetragonal 'β-Sn' phase (triangles) and the cubic diamond-like phase (squares) at ambient pressure and 100 K as at function of the average germanium content of the GaSb–Ge samples exposed to 7.5 GPa and 250°C for 24 *h*. The point for GaSb is taken from Ref. 13, that for Ge is the extrapolation of the high pressure data of Ref. 11, the other points are the data of the present work. The half-blackened symbols refer to the two-phase samples. The dashed line represents the volume dependence for the 'β-Sn' type GaSb–Ge solid solutions provided that they obey the Vegard's rule. $V_a = a^2c/4$ and $a^3/8$ for the 'β-Sn' and diamond-like phases, respectively.

The high-pressure phase of germanium is metallic and has a 'β-Sn' type crystal structure[8,11]. The high-pressure phase of the GaSb alloy is also metallic, has the same equiatomic composition as the low-pressure phase, and its crystal structure is close to that of β-Sn both under the equilibrium conditions at high pressures[8] and in a metastable state at ambient pressure and low temperatures[12,13]. Phase transformations in the GaSb–Ge alloys at high pressures were studied in Refs. 4,7. From the behaviour of the electric resistance it was concluded[7] that a homogeneous metallic phase is formed at $P > 8$–9 GPa and $T > 400$°C in the alloys with compositions in the whole range from GaSb to Ge.

As is seen from Figure 2, the high-pressure 'β-Sn' phase (called *hpp* for brevity hereinafter) was formed in all GaSb–Ge samples exposed to 7.5 GPa and 250°C in the present work. This was the only phase in the samples containing up to 30 at.% Ge, whereas the samples with 36 and 50 at.% Ge consisted of a mixture of the *hpp* and the diamond-like phase. The latter, however, was not just the rest of the low-pressure phase contained in the starting samples. The atomic volume of this phase decreased (compare Fig. 2 and Fig. 1) and now corresponded to approximately 98 at.% Ge in the GaSb–Ge solution instead of 90–93 at.% Ge before the high pressure treatment. The change in the composition of the diamond-like phase results from the effet of pressure on the limiting solid solubility of GaSb in Ge. (Note, that at least one two-phase region should seperate the region of coexistence of the sphalerite-like and the diamond-like phases from the single-phase region of the *hpp* in the equilibrium *T–P* phase diagram of the GaSb–Ge system according to the phase rule.)

In the case of the GaSb–Ge alloys containing up to 30 at.% Ge, such a two-phase region is apparently located at pressures lower than 7.5 GPa. The single phase composition of the samples of these alloys prepared at 7.5 GPa is additionally evidenced by a good agreement of the atomic volume of the quenched *hpp*, plotted as a function of the average Ge content of the alloys, with the dependence for the ideal GaSb–Ge solid solutions shown in Figure 2 with the straight line. This is the metastable *hpp* that amorphizes on heating at ambient pressure whereas the diamond-like GaSb–Ge phase with low GaSb concentration is thermodynamically stable at ambient pressure and never transforms to a metastable amorphous state. To be certain that the *hpp* sample contained no traces of the diamond-like phase, we selected the alloy with 24 at.% Ge for further investigations.

To transform the $(GaSb)_{38}Ge_{24}$ alloy to the amorphous state, the pellet of the *hpp* was heated in a PE DSC 7 differential scanning calorimeter to 150°C at a rate of 20°C/min and then cooled to room temperature at 200°C/min. The X-ray analysis revealed no traces of crystalline phases in the resultant amorphous sample. The obtained DSC curve (Figure 3) was similar to that observed earlier on amorphization of the GaSb *hpp*[13], but essentially stretched towards higher temperatures: the amorphization process in the GaSb samples was completed by the room temperature and that in the $(GaSb)_{38}Ge_{24}$ one lasted until 130–140°C. The multi-step character of this process was discussed in Refs. 13,14. The integrated exothermic heat of amorphization was the same for $(GaSb)_{38}Ge_{24}$ and for GaSb[14] and equal to 3.5 ± 0.5 kJ/mol.

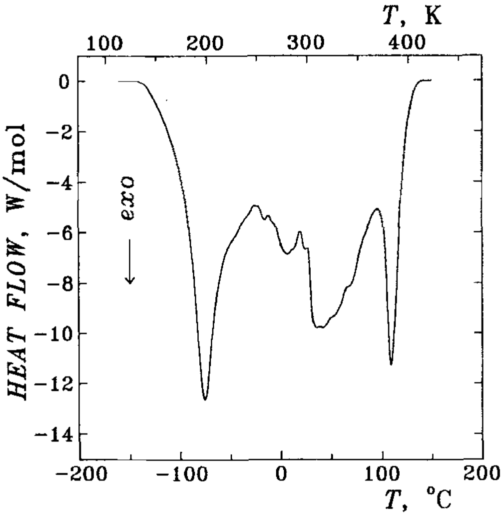

Figure 3 Heat flow versus temperature on heating the 'β-Sn' type $(GaSb)_{38}Ge_{24}$ high-pressure phase at 20°C/min in the interval of its amorphization.

According to the X-ray data of Ref. 15, the structure of a-$(GaSb)_{38}Ge_{24}$ can be represented with a continuous network of nearly ideal tetrahedra with the parameters (coordination numbers, bond lengths and angles) close to those of crystalline $(GaSb)_{38}Ge_{24}$. The density $d = 5.53 \pm 0.06\,g/cm^3$ of a-$(GaSb)_{38}Ge_{24}$ measured by hydrostatic weighing in the present work also coincided within the experimental error with $d = 5.56\,g/cm^3$ of crystalline $(GaSb)_{38}Ge_{24}$ derived from the X-ray data of Ref. 10.

The alloying with Ge strongly increases not only thermal stability of a-GaSb[7], but also its mechanical stability. Any damage or relatively light shock (say, due to a fall on the table from a height of 10 cm) results in an immediate crystallization of an a-GaSb pellet the size of a few millimeters. No traces of crystallization were observed for a-$(GaSb)_{38}Ge_{24}$ after pestling the sample to fine powder at room temperature.

The high pressure measurements of the electrical resistance were carried out on the samples in the form of bars $1 \times 1 \times 3\,mm^3$ cut from one pellet of a-$(GaSb)_{38}Ge_{24}$ with an abrasive wire saw. The resistance was measured by a conventional d.c. four-probe technique with copper electrodes pressed against the samples in Toroid type quasihydrostatic high pressure chambers using hexagonal BN as a pressure transmitting medium. The pressure was measured accurate to ±0.4 GPa, the temperature to ±7°C.

3. RESULTS

The obtained T–P diagram of phase transformations of the initially amorphous $(GaSb)_{38}Ge_{24}$ alloy is depicted in Figure 4. Representative isobars and isotherms of

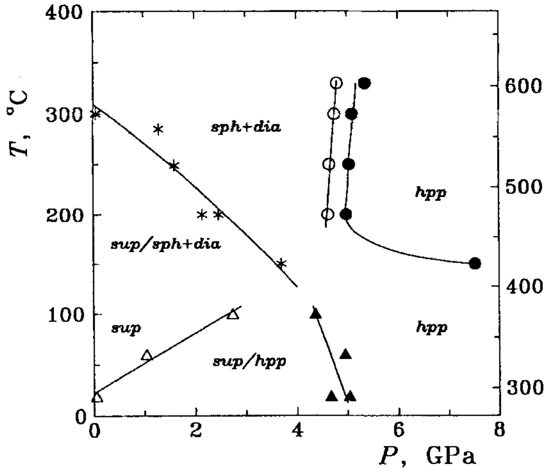

Figure 4 *T–P* diagram of phase transitions in the initially amprphous $(GaSb)_{38}Ge_{24}$. The labels: *sup* = semiconducting unordered phase; *hpp* = high-pressure '*β*-Sn' type phase; *sph* + *dia* = a mixture of the sphalerite-like and diamond-like low-pressure phases. The asterisks show the positions of the irreversible *sup*→*sph* + *dia* transition at increasing temperature or pressure. The solid and open triangles stand for the *sup*→*hpp* and *hpp*→*sup* transitions at increasing and decreasing pressure, respectively. The solid and open circles indicate the *sph* + *dia*→*hpp* and *hpp*→*sph* + *dia* transitions, also at increasing and decreasing pressure.

electrical resistance used to construct this diagram are shown in Figures 5 and 6. The phase identification in the fields labelled in Figure 4 was determined by X-ray examination of the quenched samples. The labels with slashes mark the fields where either of the indicated phase compositions was possible depending on the previous treatment. Phase transformations in the samples never heated above 100°C were qualitatively different from the transformations observed at higher temperatures that allows one to consider the *T–P* diagram in Figure 4 as composed of two separate parts, below and above 100°C. The labelling of the fields in Figure 4 takes account of this separation. The amorphous state is called the semiconducting unordered phase (*sup*) because the latter is more suitable for further discussion in Section 4.

As is seen from the upper part of Figure 4, the crystallization temperature of the amorphous $(GaSb)_{38}Ge_{24}$ to the *sph* + *dia* mixture decreased from about 300°C at ambient pressure (which agrees with the data of Ref. 7) to about 150°C at 3.7 GPa. The hysteresis of the *sph* + *dia*⇄*hpp* transformation was small and lied within the experimental error at $T \geqslant 200$°C, and the curve of the transformation was close to the vertical line $P = 5$ GPa. The formation pressure of the *hpp* steeply increased with the decrease in temperature to 150°C, and no transformations occurred in the *sph* + *dia* samples at lower temperatures and $P \leqslant 7.7$ GPa.

At $T \leqslant 100$°C, the *a*-$(GaSb)_{38}Ge_{24}$ crystallized to the *hpp* at pressures above 4.5–5 GPa. The *hpp* samples, however, contained traces of the low pressure *sph* and *dia*. The *sup*→*hpp* transformation was reversible, and the pressure of amorphization of the *hpp* increased from nearly atmospheric pressure at 17°C to 2.7 GPa at 100°C. The obtained amorphous samples also contained traces of the *sph* and *dia*. The lines

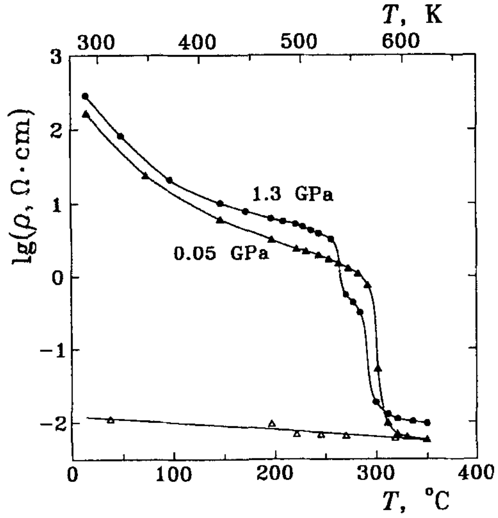

Figure 5 Isobars of the electrical resistivity, ρ, measured on step-wise heating (solid symbols) and cooling (open symbols) of the amorphous $(GaSb)_{38}Ge_{24}$ samples.

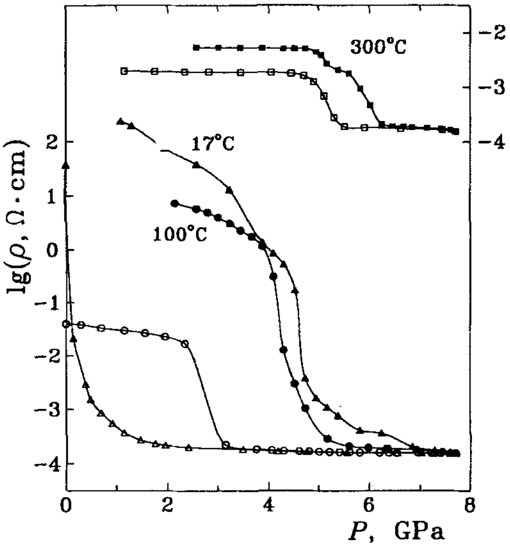

Figure 6 Isotherms of the electrical resistivity, ρ, of the initially amorphous $(GaSb)_{38}Ge_{24}$ samples measured in the course of a step-wise increase (solid symbols) and decrease (open symbols) in pressure.

of the *sup*→*sph*+*dia* and *sup*→*hpp* transformation seem to form a continuous and rather smooth boundary of the *sup* existence region in the *T–P* diagram.

As is seen from the comparison of the phase compositions of the adjacent fields in Figure 4 at $T >$ 100°C, direct transitions betwen the fields are inconsistent with the phase rule. The points in Figure 4 actually show the centres of the finite temperature or pressure intervals involving two or more phase transitions. Because of the different rate of these transitions, they can be noticeably spaced apart and clearly seen if the temperature or pressure is changed quickly enough. For example, in the course of the DTA measurement at ambient pressure[7] with a heating rate of 20°C/min, the amorphous $(GaSb)_{\approx 38}Ge_{\approx 24}$ alloy first transformed at about 300°C to another metastable state, a homogeneous sphalerite-like solid solution, which then decomposed to a nearly equilibrium mixture of the sphalerite-like (*sph*) and diamond-like (*dia*) phases, depleted and enriched in germanium.

In the present work, the temperature and pressure dependences of electrical resistivity, ρ, were measured at a step-wise increase or decrease in temperature or pressure. The samples were exposed at each given point until the slope of the $\lg(\rho)$ versus time dependence decreased by a factor of ten, and the final value of $\lg(\rho)$ was plotted in the figure. At any temperature from 17 to 330°C, this took 40–90 min in the vicinity of the phase transformations and 5–20 min in the other intervals. As is seen from Figures 5 and 6, with the changes in the temperature and pressure that slow, the intervals of complex phase transformations between the fields labelled in Figure 4 are rather narrow, the different stages of the transformations are not well resolved and apparently overlap. Accordingly, it did not seem useful showing these intervals in the T–P diagram.

The transformation of a-$(GaSb)_{38}Ge_{24}$ to the *sph* + *dia* mixture (asterisks in Fig. 4) was accompanied by a fall of the resistivity, see Figure 5. Sometimes this was a single rather steep step of the dependence as in the isobar at 0.05 GPa, sometimes the behaviour of the resistivity was more complicated reflecting a multi-stage character of the transformation as in the isobar at 1.3 GPa. Every time the transformation was irreversible. This fact was evidenced by the X-ray data as well as by the behaviour of the resistivity (compare the dependences at 0.05 GPa measured on heating and on cooling). Judging by the V_a values, the resultant *sph*+*dia* mixture consisted of the sphalerite-like phase containing about 2.5 at.% Ge and the diamond-like phase with about 96 at.% Ge. The composition of the samples was thus close to the thermodynamically equilibrium one at low pressures[9], so they had no reason to transform back to the metastable amorphous phase.

After the transformation of the a-$(GaSb)_{38}Ge_{24}$ sample to the *sph*+*dia* state was completed, the temperature was set to a certain chosen value and the isotherm of electrical resistance was measured at increasing and then at decreasing pressure in order to determine the positions of the *sph*+*dia*→*hpp* and *sph*+*dia*←*hpp* transformations. A representative isotherm at 300°C is given in Figure 6. The obtained positions of the transformations are shown in Figure 4 by the circles.

In contrast to the *sup*→*sph*+*dia* transformation, both initial and final states of the *sph*+*dia*→*hpp* transformation are thermodynamically equilibrium. To answer the phase rule, the interval of this transformation should incorporate at least two different phase regions as the initial and final states of the transformation differ by two phases. As was discussed in the previous Section, a *dia*+*hpp* field exists in the equilibrium T–P diagrams of $(GaSb)_{32}Ge_{36}$ and $(GaSb)_{25}Ge_{50}$ alloys. The diagram of the $(GaSb)_{38}Ge_{24}$ alloy is most probably of the same type and hence also contains the *dia*+*hpp* field which adjoins the *hpp* field. Then the simplest sequence of the phase fields crossed during the phase transformation is *sph*+*dia*→*sph*+*dia*+*hpp*→*dia*+*hpp*→*hpp*.

In the interval of the *sph*+*dia*→*hpp* transformation at increasing pressure, two steps were always seen in the isotherms of the electrical resistance (Figure 6, curve 300°C, solid squares). The first of this steps is thus reasonable to ascribe to the transition of the Ge-depleted *sph* to the *hpp*, and the second step to the dissolution of the Ge-rich *dia* in the formed *hpp*. The intervals of these transitions, however, seem to noticeably overlap as the first step is too small, so the fully equilibrium *sph*+*dia*+*hpp* and *dia*+*hpp* states were not reached in the experiment. Judging by the presence of only one step in the electrical resistance isotherms measured at decreasing pressure (Fig. 6, curve 300°C, open squares), the reverse transitions occurred practically simultaneously.

Proceeding to the lower part of Figure 4, note that the points of the *sup*→*hpp* transformation are located very close to the linear prolongation of the nearly vertical line of the *sph*+*dia*⇄*hpp* transformation at $200 \leqslant T \leqslant 330$°C. The *hpp* therefore was mainly formed in the region of its stability in the equilibrium *T*–*P* diagram. The quenched *hpp* samples, however, contained traces of the low-pressure *sph* and *dia*. The low-pressure phases might be formed on crossing the *sph*+*dia*+*hpp* and *dia*+*hpp* intervals of the *sph*+*dia*→*hpp* transformation at increasing pressure as the interval of the *sup*→*hpp* transformation was large enough to cover both of them (see Fig. 6, curves 17°C and 100°C, solid symbols). These phases did not transform to the *hpp* at higher pressures due to a large hysteresis of the *sph*+*dia*→*hpp* transformation at temperatures below 200°C which is clearly seen in the upper part of Figure 4.

The above *sph* and *dia* being stable phases at low pressures, undoubtedly remained in the samples after the reverse *hpp*→*sup* transformation occurring on decreasing pressure at $T \leqslant 100$°C. The fraction of the *sph* and *dia*, however, noticeably increased, so the *hpp* had partly transformed to a mixture of these phases. The latter agrees with the observations in Ref. 7 that the amorphous GaSb and GaSb–Ge samples containing up to 25 at.% Ge and produced by decompression of the *hpp* at room temperature, always contained about 10 vol.% of crystalline phases. If the *hpp* sample was decompressed at −170°C, no formation of the crystalline phases in the course of the *hpp*→*sup* transformation on further heating at ambient pressure was observed for $(GaSb)_{38}Ge_{24}$ in the present work (this is how the initial amorphous sample was prepared) and for GaSb in Refs. 12,13.

Another difference between the $(GaSb)_{38}Ge_{24}$ samples decompressed at −170°C and then heated at ambient pressure and those decompressed at room and higher temperatures in the high pressure chamber was that the former still contained a noticeable amount of the *hpp* even after heating above 100°C whereas the latter never contained any traces of this phase. We attribute this to additional plastic deformation of the samples faciltating the *hpp*→*sup* transformation during decompression of the quasihydrostatic high pressure chamber at elevated temperatures. The X-ray examination showed that the partly amorphous $(GaSb)_{38}Ge_{24}$ sample obtained by heating the quenched *hpp* to room temperature at ambient pressure transformed to the fully amorphous state after pestling in the mortar.

4. DISCUSSION

4.1. *T–P Diagram of Metastable 'Isoconcentrational' Equilibria in the $(GaSb)_{38}Ge_{24}$ System*

The available models relate the phenomenon of pressure induced solid state amorphization (SSA) to specific features of the *T–P* diagrams of stable and metastabel equilibria involving the crystalline phases[6]. The *T–P* diagram needed for the discussion of the effect of pressure and temperature on the phase transformations of *a*-$(GaSb)_{38}Ge_{24}$ is actually the diagram of metastable 'isoconcentrational' equilibria between the phases with a fixed $(GaSb)_{38}Ge_{24}$ composition. In fact, the amorphous state is formed from and transforms to the phases with this composition only. As is seen from Figure 4, at $T \leqslant 100°C$ this is the *hpp* (the small amount of the equilibrium *sph* and *dia* phases precipitating in the course of the *sph*→*hpp* and *hpp*→*sup* transformations practically does not change the composition of the resultant *hpp* and *sup*). At $T > 100°C$ this is the semiconducting homogeneous sphalerite-like $(GaSb)_{38}Ge_{24}$ solid solution (low pressure phase, *lpp*, hereafter) which forms first in the course of the irreversible *sup*→*sph*+*dia* transformation[7].

The metastable *T–P* diagram of phase equilibria in the quasi one-component $(GaSb)_{38}Ge_{24}$ system cannot be obtained directly in experiment, but it can be outlined on the basis of the data accumulated for the Ge, GaSb and GaSb–Ge systems.

The experimental *T–P* diagram of stable equilibria in Ge is shown in Figure 7 by solid lines. The diagram is characterized by a triple point (9.5 GPa, 500°C) of the

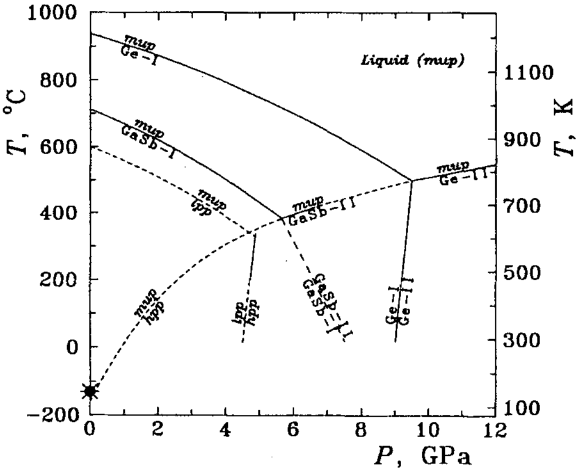

Figure 7 Experimental *T–P* diagrams of stable equilibria in Ge (shown by the solid lines, Ref. 8) and GaSb (the melting curve is shown solid, the GaSb-I ⇄ GaSb-II line is shown dashed as it is not determined correctly yet, Ref. 8) and a tentative *T–P* diagram of the metastable 'isoconcentrational' equilibria in the $(GaSb)_{38}Ge_{24}$ system, see text. The sun-like symbol marks the temperature at which amorphization of the quenched $(GaSb)_{38}Ge_{24}$ *hpp* begins at ambient pressure. The labels: *mup* = metallic unordered phase, either liquid or amorphous; *lpp* = low-pressure sphalerite-like $(GaSb)_{38}Ge_{24}$ phase; *hpp* = high-pressure '*β*-Sn'-like $(GaSb)_{38}Ge_{24}$ phase; Ge-I and GaSb-I are the low-pressure diamond-like phases; Ge-II and GaSb-II are the high-pressure '*β*-Sn'-like phases.

equilibrium among the semiconducting low-pressure Ge-I phase, the metallic high-pressure Ge-II phase and the metallic liquid. The latter is called, as in Ref.16, a metallic unordered phase (*mup*) so that the same name can further be used for this phase when it is in the equilibrium liquid state as well as in the undercooled liquid and amorphous states. The experimental T–P diagram of GaSb, also presented in Figure 7, is an analogue of the Ge diagram with the triple point being shifted to lower pressure and temperature (5.65 GPa, 385°C). One could expect that the 'isoconcentrational' T–P diagram of a Ge and GaSb solid solution should be of the same type.

The 'β-Sn'-like Ge-II and GaSb-II high-pressure phases belong to one homological sequence[17] and the pressure dependences of their melting points well fit one smooth curve shown dashed in Figure 7. The 'β-Sn'-like $(GaSb)_{38}Ge_{24}$ *hpp* belongs to the same homological sequence as the Ge-II and GaSb-II phases, so the pressure dependence of its 'isoconcentrational' melting point should fall onto the same dashed curve in Figure 7.

The temperature $T_0 = 600°C$ of the 'isoconcentrational' melting of the $(GaSb)_{38}Ge_{24}$ *lpp* at ambient pressue was calculated in Ref. 10. The $lpp \rightleftarrows mup$ curve in Figure 7 was plotted equidistantly relative to the GaSb-I$\rightleftarrows$*mup* melting curve. The line of the $lpp \rightleftarrows hpp$ metastable equilibrium was roughly approximated by the $sph + dia \rightleftarrows hpp$ line (the solid portion of this line is drawn through the middle of a rather narrow interval between the hysteresis branches at $200 \leqslant T \leqslant 330°C$, Figure 4).

As is seen from Figure 7, the three lines, $hpp \rightleftarrows mup$, $lpp \rightleftarrows mup$ and $lpp \rightleftarrows hpp$, intersect approximately at one point at around 5 GPa and 350°C. This evidences that the above assumptions concerning the type of the 'isoconcentrational' T–P diagram of $(GaSb)_{38}Ge_{24}$ and the positions of the boundary lines were rather correct and self consistent.

The 'isoconcentrational' diagram of $(GaSb)_{38}Ge_{24}$ is thus an analogue of those for Ge and GaSb. With the T–P diagrams of this type, spontaneous solid state amorphization of the high pressure phase is usually associated with the loss of its thermodynamic stability with respect to the long-range order when the phase crosses its extrapolated melting curve at a temperature which is low enough to suppress transformations to other crystalline modifications. This hypothesis of 'cold melting' was first formulated by Mishima *et al.*[18] who observed SSA of the I_{VIII} high-pressure phase of ice on crossing its extrapolated melting curve at decreasing pressure as well as SSA of the I_{h} low-pressure modification of ice on crossing its extrapolated melting curve at increasing pressure. Richet[19] used these considerations to explain SSA of silicates. Later the hypothesis of 'cold melting' as a cause of pressure-induced SSA was adopted and widely used by many researchers including the authors of the present paper.

At ambient pressure, the amorphization of the $(GaSb)_{38}Ge_{24}$ *hpp* begins at a temperature of about $-130°C$ as indicated in Figure 7 by the sun-like symbol. To agree with the 'cold melting' hypothesis, the melting curve of the *hpp* was extrapolated so as to cross the y-axis below this temperature.

The obtained 'isoconcentrational' T–P diagram of $(GaSb)_{38}Ge_{24}$ is depicted in Figure 8 by the solid lines, the $lpp \rightleftarrows mup$ line being slightly changed compared with that in Figure 7 in order to intersect with the $hpp \rightleftarrows mup$ and $lpp \rightleftarrows hpp$ lines at one point.

The lengthy discussion of the 'isoconcentrational' phase equilibria in the $(GaSb)_{38}Ge_{24}$ system was a sort of a payment for the possibility to have a more thermally and mechanically stable amorpous state allowing investigations within a wide temperature and pressure interval. Let us consider now what new information can be derived from the results of such an investigation.

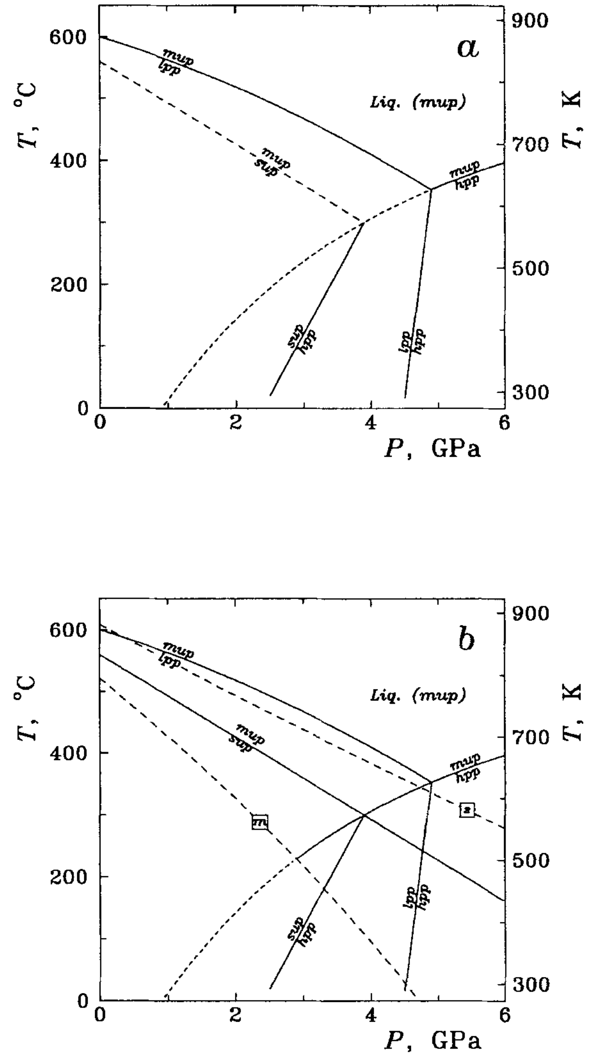

a

b

Figure 8a, b, c, d T–P diagram of the metastable 'isoconcentratinal' phase equilibria (extrapolated and calculated curves) and phase transformations observed in experiment (marked with symbols) in the $(GaSb)_{38}Ge_{24}$ system. The labels *sup*, *mup*, *lpp* and *hpp* denotes the same phases as in Figures 4 and 7; the asterisks and triangles have the same meaning as in Figure 4. The dashed lines labelled '*s*' and '*m*' show the boundaries of themodynamics stability of the *sup* and *mup*, respectively.

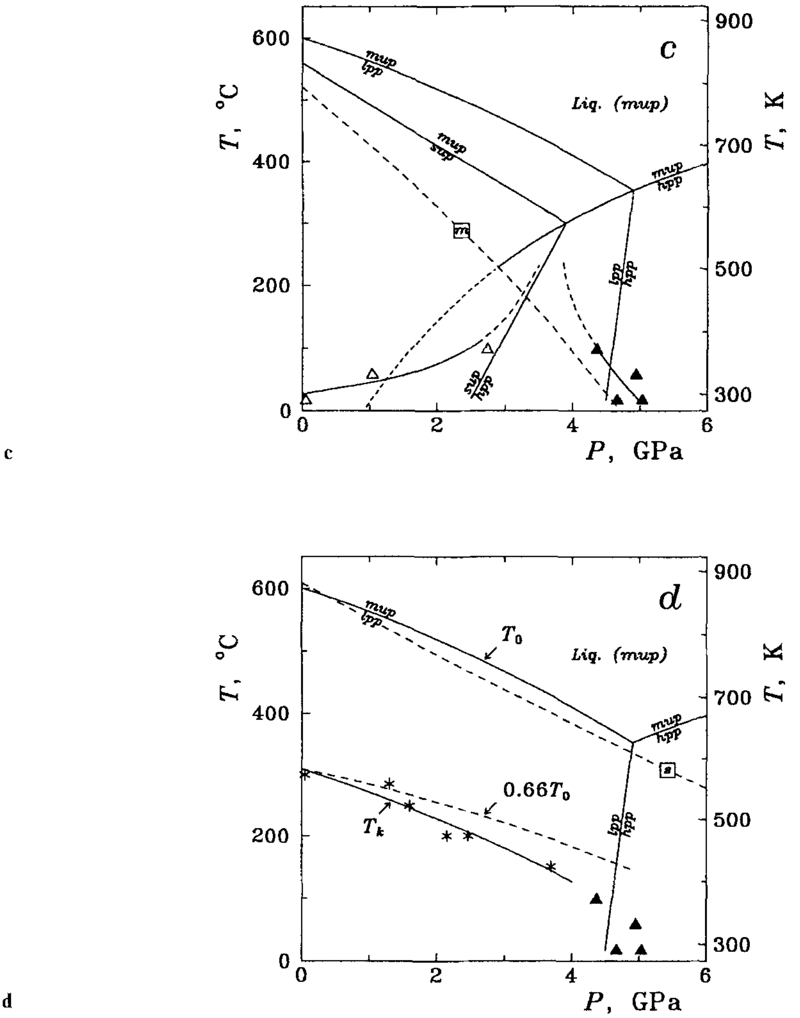

Figure 8 (*Continued*).

4.2. *Metastable Equilibria Involving the Semiconducting Unordered Phase*

As is seen from Figure 4, the *sup*$\rightleftarrows$*hpp* transformation in $(GaSb)_{38}Ge_{24}$ at $T \leqslant 100°C$ appears as a typical first order phase transformation: it is reversible and exhibits the hysteresis decreasing with increasing temperature. This is possible only in the case when each of the final states of the transformation is a phase, *i.e.* the state corresponding to a minimum of the thermodynamical potential at given external parameters. The amorphous state in the $(GaSb)_{38}Ge_{24}$ system is thus a classic phase, though a metastable one, and not just a 'frozen' intermediate state. To emphasize this fact and by analogy with the *mup*, we call it the semiconducting unordered phase (*sup*) in this paper.

As both *sup* and *hpp* are phases, a line of the *sup*⇄*hpp* equilibrium should pass somewhere between the *sup*→*hpp* and *hpp*→*sup* lines in the T–P diagram of $(\mathrm{GaSb})_{38}\mathrm{Ge}_{24}$. The available experimental data allow one to determine the position of this line more accurately.

The slope of an equilibrium line should follow Clapeyron equation $dT/dP = T\Delta V/\Delta H$, where ΔV and ΔH are the differences between the volumes and enthalpies of the two phases in equilibrium at given T and P (if not specified, the temperature is in Kelvins hereafter). The integral heat of the *hpp*→*sup* transition in $(\mathrm{GaSb})_{38}\mathrm{Ge}_{24}$ measured at ambient pressure is $\Delta H^{\circ}(300\,\mathrm{K}) \approx +3.5\,\mathrm{kJ/mol}$ (we refer this value to $T \approx 300\,\mathrm{K}$ as it is the center of the temperature interval of the transition, see Fig. 3). Let the pressure of the *sup*⇄*hpp* equilibrium at 300 K is $P = 2.5\,\mathrm{GPa}$, which is the center of the hysteresis interval at this temperature (Fig. 4). The ΔH value at $T = 300\,\mathrm{K}$ and $P = 2.5\,\mathrm{GPa}$ then can be estimated as:

$$\Delta H \approx \Delta H^0 + P\left(\frac{\partial H}{\partial P}\right)_T = \Delta H^0 + P\left[\Delta V - T\left(\frac{\partial \Delta V}{\partial T}\right)_P\right] \approx \Delta H^0 + P\Delta V.$$

With $V_{sup} = 16.3\,\mathrm{cm}^3/\mathrm{mol}$ and $V_{hpp} = 13.2\,\mathrm{cm}^3/\mathrm{mol}$ from the density and X-ray measurements at ambient pressure this yields:

$$\Delta V \approx -3.1\,\mathrm{cm}^3/\mathrm{mol};\quad \Delta H \approx +3.5 - 8 = -4.5\,\mathrm{kJ/mol} \text{ and } dT/dP \approx +200\,\mathrm{K/GPa}.$$

The *sup*⇄*hpp* line with this slope is erected in Figure 8a. As is seen, it intersects the *hpp*⇄*mup* line at about 3.9 GPa and 570 K. In accordance with the phase rule this intersection should be a triple point and give birth to the third line, the line of the *sup*⇄*mup* equilibrium.

The line of the *sup*⇄*mup* equilibrium is a new element for the T–P diagrams with semiconducting amorphous phases. As a line of the metastable equilibrium, it extends on both sides of the triple point (Fig. 8b) and describes equilibrium between the *sup* and *mup* which can be considered as either liquid or solid (*i.e.* amorphous) phases depending on their viscosity at a given temperature. The *sup*⇄*mup* line has never been observed in experiment, but its existence and approximate position was predicted for the GaSb, InSb and InAs systems as a result of the model calculations[16].

In the case of the $(\mathrm{GaSb})_{38}\mathrm{Ge}_{24}$ system one point of the *sup*⇄*mup* line is known and the position of this line can be determined prior to model calculations and more accurate than for the systems considered in Ref. 16. In fact, the slope of this line, $dT/dP = T\Delta V/\Delta H = \Delta V/\Delta S$, where S is the entropy, should be negative because $\Delta S > 0$ and $\Delta V < 0$ when any covalent substance melts to a metallic liquid[16,20]. Moreover, the value of ΔS should be of the order of 30 J/(K·mol) if the substance is a covalent compound, and the value of ΔV should not differ much from that for the *sup*⇄*hpp* transformation[16]. This yields dT/dP of the order of $-100\,\mathrm{K/GPa}$. The *sup*⇄*mup* line with $dT/dP = -100\,\mathrm{K/GPa}$, however, would intersect the *lpp*⇄*mup* line at about 1.5 GPa. This does not look probable because it means that a metal-to-semiconductor transition should occur in the $(\mathrm{GaSb})_{38}\mathrm{Ge}_{24}$ melt at ambient pressure whereas the melts of various diamond-like and sphalerite-like semiconductors studied at ambient pressure were shown to be metals with low concentration of semiconducting clusters at temperatures down to the melting point[21].

One can see therefore that the mutual position of the equilibrium lines in the metastable *T–P* diagram of $(GaSb)_{38}Ge_{24}$ strictly confines allowable values of the slope of the *sup⇄mup* line. The *sup⇄mup* line plotted in Figure 8 has $dT/dP = -70$ K/GPa that corresponds to $\Delta S \approx 44$ J/(K·mol).

4.3. Model Calculations

To know more about the *sup⇄mup* equilibrium, a model is necessary. We will use the two-level model first developed to describe the *T–P* diagram of cerium undergoing an isomorphic transition[22] and then successfully applied to the transitions between amorphous phases in ice[23] and GaSb, InSb and InAs alloys[16].

The basic concept of this model is that both *mup* and *sup* are formed by the clusters of two types, metallic and semiconducting, which are considered as two microscopic states or two components of the unordered system. The Gibbs potential of the system is then written in the approximation of regular solutions:

$$G = G_m C + G_s(1-C) + UC(1-C) + RT[C \ln C + (1-C)\ln(1-C)], \qquad (1)$$

where G_m and G_s are the Gibbs potentials of the components, *i.e.*, of the alloy in purely metallic and semiconducting unordered states, U is the mixing energy and C is the volume concentration of the metallic component. By contrast to the standard approximation of regular solution, the parameter C is not an independent variable; it is found from the minimum conditions:

$$\partial G/\partial C = 0; \quad \partial^2 G/\partial C^2 > 0.$$

As a function of C, the Gibbs potential (1) can have one or two minima depending on the *T–P* region involved[24]. The two minima of $G(C)$ are equal along a straight line which is the line of the first order transformation between the *mup* and *sup*. Along this line, the concentration of the metallic clusters increases in the *sup* and decreases in the *mup* with increasing temperature, and the line terminates at a critical point at $T_{cr} = U/2R$. The points in the *T–P* plane where one of the two minima of $G(C)$ degenerates to an inflection point, form the line of a complete loss of thermodynamic stability of the corresponding phase; the two lines formed in this way terminate at the same critical point with the *sup⇄mup* equilibrium line.

The Gibbs potential (1) is specified in a unique fashion by four constants: U and ΔE, ΔS and ΔV which are the differences between the internal energies, entropies and volumes of the components. In the case of the $(GaSb)_{38}Ge_{24}$ system, ΔV was set equal to 3.1 am^3/mol and then $\Delta E = 36.2$ kJ/mol and $\Delta S = 44$ J/(K·mol) were determined from the position of the *sup⇄mup* line shown in Figure 8a. The value of $U = 19$ kJ/mol was chosen so that $C = 92$ vol.% at ambient pressure and 873 K which is the point of 'isoconcentrational' melting of the *lpp*. This concentration of the metallic component was observed[21] at the melting temperature in liquid GaSb, the nearest analogue of $(GaSb)_{38}Ge_{24}$. With the chosen value of U, the line of ths *sup⇄mup* equilibrium terminates at a critical point at about 1140 K and a negative pressure of about -4.3 GPa.

So far as the phase equilibria are concerned, the most interesting result of the model calculation is the position of the lines where the *sup* and *mup* lose their thermodynamic stability. These lines are shown dashed in Figure 8b and superimposed on the equilibrium diagram. The *sup* is no longer a phase above the line labelled '*s*' and the *mup* cannot exist below the line labelled '*m*'.

4.4. *Effects Caused by Phase Instability*

The position of the boundaries of thermodynamic stability of the *sup* and *mup* in the *T–P* diagram of $(GaSb)_{38}Ge_{24}$, though determined rather semi-quantitatively, allows some distinct conclusions.

4.4.1. *Position of the 'm' line*

It explains, for example, why the quenched *hpp* does not transform to a metallic amorphous state on heating at ambient pressure: this state just does not correspond to any minimum of the thermodynamic potential at temperatures up to about 800 K.

The position of the '*m*' line also explains why no amorphous state of $(GaSb)_{38}$ Ge_{24} has ever been obtained by quenching from the melt at ambient pressure: the metallic melt becomes unstable and inevitably transforms to some other state at a rather high temperature, above 800 K; the cooling rate slows down because of the heat release accompanying the transformation, and this allows crystallization of the alloy.

Another interesting feature of the diagram is that the line of the metastable *hpp*⇄*mup* equilibrium cannot extend below the '*m*' line because the *mup* does not exist there as a phase. The *hpp*⇄*mup* line therefore terminates at a critical point on intersection with the '*m*' line at about 500 K and 3 GPa.

This critical point is of a new type never analyzed before. In particular, physical sense (if any) of the *hpp*⇄*mup* line extrapolated below the critical point is not clear at the present. This problem, however, is worth discussing as the extrapolation of the melting curve of the high pressure phase to low temperatures and pressures has been successfully used to explain the phenomenon of spontaneous amorphization in a number of different systems[6].

4.4.2. *Melting curve of the hpp and hysteresis of the sup⇄hpp transformation*

It seems well established that the melting temperature of a solid is close to the temperature of its thermodynamic instability (an adequate bibliography concerning melting and instability of the crystals with respect to long range order is given in Ref. 25). One can assume therefore that the *hpp*⇄*mup* line itself (shown solid in Fig. 8b) and its smooth extrapolation below the critical point (shown dashed in Fig. 8b and to lower temperatures in Fig. 7) represent the boundary of thermodynamical stability of the *hpp*. It is exactly the idea exploited to account for amorphization of the high pressure phase on crossing its extrapolated melting curve at low temperature and pressure[16]. In the case of the $(GaSb)_{38}Ge_{24}$ system, however, this idea does not work.

Figure 8c presents the hysteresis branches of the *sup*⇄*hpp* transformation determined in the experiment. As is seen, the line of the *hpp*→*sup* transition intersect the extrapolated *hpp*$\rightleftarrows$*mup* line at a rather high pressure of about 1 GPa. This cannot happen if the *hpp* does not exist on the left of the *hpp*$\rightleftarrows$*mup* line. The behaviour of the *hpp*$\rightarrow$*sup* line thus allows a conclusion that the boundary of the *hpp* stability region lies above room temperature at the pressures down to few hundred atmospheres and therfore much differs from the extrapolated *hpp*$\rightleftarrows$*mup* line at least for $P < 1$ GPa.

The intersection of the *hpp*$\rightarrow$*sup* line with the extrapolated *hpp*$\rightleftarrows$*mup* line also shows that the loss of thermodynamic stability of the crystalline phase is not a necessary condition for its amorphization. For example, at 473 K the *hpp* transforms to the *sup* at about 2.7 GPa (the rightmost open triangle in Fig. 8c), deeply inside the region where the *hpp* can exist as a phase according to the discussion above.

Summing up, it can be concluded that at temperatures above 290 K the *sup* appears as a usual metastable phase. Its formation is thermodynamically possible under the conditions determined by the line of the *hpp*$\rightleftarrows$*sup* equilibrium and not by the melting line of the *hpp* extrapolated from higher temperatures as it was often thought before.

As for the reverse *sup*$\rightarrow$*hpp* transformation, it takes place near the '*m*' line. If it is not just a coincidence, this might suggest that the *mup* forms in the course of the *sup*$\rightarrow$*hpp* transformation as an intermediate state (still amorphous, but already metallic) promoting the reaction. Note, however, that the $\Delta G \approx P\Delta V$ contribution to the thermodynamic driving force of the *sup*$\rightarrow$*hpp* (and *sup*$\rightarrow$*mup*) transformation is large and rapidly increases with the pressure due to the large $\Delta V \approx -20\%$ of the transformation. This should decrease the pressure hysteresis of the *sup*$\rightleftarrows$*hpp* transformation by increasing the steepness of its *sup*$\rightarrow$*hpp* branch in no dependence of the specific transformation mechanism.

4.4.3. *Thermal stability of the sup*

An interesting effect is a rather steep decrease, by about 150 K at 3.7 GPa, in the temperature T_k of the *sup* crystallization to the *lpp*, see Figure 8d. The *sup*$\rightarrow$*lpp* transformation is accompanied by a small change in volume, less than 1%, so the $\Delta G \approx P\Delta V$ contribution to the thermodynamic driving force can hardly explain the observed pressure effect.

The *sup*$\rightarrow$*lpp* line, however, is not a line of a thermodynamic equilibrium. Its position in the T–P diagram is also affected by kinetical factors, actually determined by the energy barriers retarding redistribution of the atoms in the course of the transformation, and the effectiveness of the barriers is characterized by thermal stability of the initial and final products of the transformation.

As a measure of thermal stability of the solids (the value of self-diffusion coefficient, *etc.*) and of various states of the solids (the recrystallization temperature of microcrystalline or strongly deformed or amorphous materials, *etc.*), the reduced temperature, T/T_m is usually used, where T_m is the melting temperature of the equilibrium crystalline phase. In particular, the so-called Kauzmann rule works well for a large group of semiconducting materials[26]. According to this rule, $T_g/T_m \approx 2/3$, where T_g is the glass transition temperature of the melt which is usually close to the crystallization temperature of the resultant amorphous state.

For the $(GaSb)_{38}Ge_{24}$ at ambient pressure, the ratio $T_k/T_0 = 573/873 \approx 0.66 \approx 2/3$, where T_0 is the temperature of 'isoconcentrational' melting of the crystalline *lpp*. The Kauzmann rule is thus well satisfied. If this rule is applicable to the $(GaSb)_{38}Ge_{24}$ at high pressures, the 'Kauzmann' contribution to the $T_k(P)$ dependence will be represented by the line $T(P) = 0.66 \cdot T_0(P)$. This line is plotted dashed in Figure 8d and accounts for about two-third of the pressure effect on the T_k at $P = 3.7$ GPa.

It is a good accuracy for the description of the pressure behaviour of a non-equilibrium parameter. For example, the positions of the hysteresis branches of any first order phase transition (say *sup*$\rightleftarrows$*hpp*) usually cannot be predicted even qualitatively. We believe therefore that the melting curve of the equilibrium semiconducting phase can be a good guide for evaluation of the pressure effect on thermal stability of the related amorphous state.

The $(GaSb)_{38}Ge_{24}$ systems gives one more example in support of the said: it is seen from Figure 8d that the '*s*' line, the boundary of the *sup* stability region, is practically parallel to the $T_0(P)$ line.

Another example is the pressure dependence of the crystallization temperature of amorphous selenium[2] depicted in Figure 9. The dependence shows a pronounced maximum at a pressure of 1–1.5 GPa though the transformation is accompanied by a large volume decrease[26] of about 11% that should have led to a monotonous and steep decrease in the T_k with increasing pressure. The melting temperature of trigonal Se-I, a crystalline analogue of *a*-Se, however steeply increases with the pressure that, as we suggest, indicates an increase in the thermal stability of *a*-Se. The two opposite effects are of the same order of magnitude as their competition gives rise to the $T_k(P)$ dependence with a maximum.

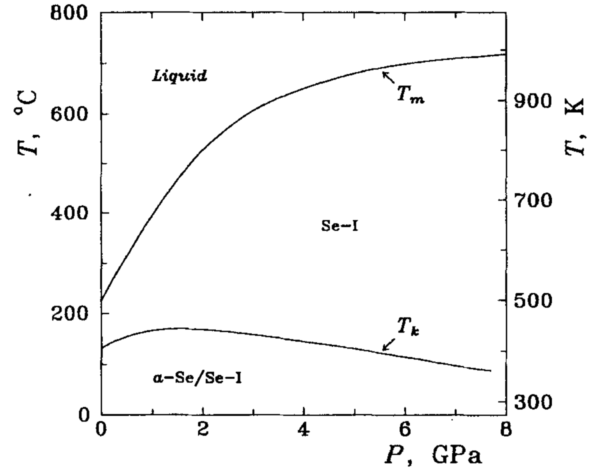

Figure 9 Pressure dependences of the crystallization temperature, T_k, of amorphous selenium[2] and of the melting temperature, T_m, of the crystalline Se-I phase[27].

5. CONCLUSIONS

By using the method of spontaneous amorphization of the metastable high-pressure phase on heating at ambient pressure, a bulk sample of amorphous semiconductor $(GaSb)_{38}Ge_{24}$ was prepared. The sample contained no crystalline inclusions and demonstrated the highest thermal and mechanical stability of all amorphous materials produced so far by this method^5.

The crystallization temperature of a-$(GaSb)_{38}Ge_{24}$ was shown to monotonously decrease with applying pressure from 300°C at ambient pressure to room temperature at about 5 GPa. In accordance with the T–P diagram of stable equilibria also measured in the present work, the crystallization products were either the metallic high-pressure phase (*hpp*) at $T \leqslant 100°C$ or a mixture of the semiconducting low-pressure phases at higher temperatures. The crystallization was reversible in the first case and irreversible in the second.

The analysis of the available experimental data and the model calculations showed that a-$(GaSb)_{38}Ge_{24}$ is a metastable phase (not just a 'frozen' non-equilibrium intermediate state) and allowed a construction of the T–P diagram (Fig. 8b) of metastable equilibria between this semiconducting unordered phase (*sup*), the *hpp* and the metallic unordered phase (*mup*). In the diagram, both *sup* and *mup* can be considered as either amorphous or liquid phases depending on their viscosity at a given temperature.

Amorphization of the high-pressure phase at decreasing pressure was shown to be thermodynamically possible under the conditions determined by the line of the $hpp \rightleftarrows sup$ equilibrium and not by the melting curve of the *hpp* (the line of the $hpp \rightleftarrows mup$ equiblirium) extrapolated from higher temperatures, as it was often thought before. The conditions of the *sup* formation (open triangles in Figure 8c) do not correlate with the position of the *hpp* melting curve either.

Moreover, the region where the *mup* can exist as a phase, *i.e.* as a state corresponding to a minimum of the thermodynamic potential, was shown to be bound from below (the '*m*' line in Fig. 8c). The *hpp* melting curve terminates at a critical point on intersection with this boundary and cannot be extended to lower temperatures.

The steep decrease in the temperature of the irreversible crystallization of the *sup* at pressures to about 3.7 GPa accompanied by a small volume effect was attributed to the decrease in thermal stability of the *sup* and the homogeneous sphalerite-like $(GaSb)_{38}Ge_{24}$ solid solution which is the first product of the crystallization. The behaviour of the melting curve of the crystalline semiconducting phase was suggested as a guide for evaluating the pressure effect on thermal stability of the related amorphous phase.

The above features are expected to be typical for phase transformations in many other substances (Ge, Si, C, GaSb, Cd–Sb, Zn–Sb, *etc.*) characterized by a decrease in the melting temperature of the low-density phase with increasing pressure.

Acknowledgments

The work was supported by the Grants No. 96-02-18545 and No. 96-02-17486 from the Russian Foundation for Basic Research.

References

1. O. Shimomura, S. Minomura, N. Sakai, K. Asaumi, K. Tamura, J. Fukushima and H. Endo, Pressure-induced semiconductor-metal transitions in amorphous Si and Ge, *Phil. Mag.*, **29**, 547 (1974).
2. K. Tamura, M. Mushiage and H. Endo, Semiconductor-metal transition and structural modification in amorphous Se-Te mixtures under high pressure, in: *Solid State Physics under Pressure*, ed. S. Minomura [KTK Scientific Publishers, Tokyo, 1985], p. 291.
3. K. Asaumi, O. Shimomura and S. Minomura, Pressure-induced structural transforamtions in amorphous InSb, *J. Phys. Soc. Japan*, **41**, 1630 (1976).
4. V. A. Sidorov, V. V. Brazhkin, L. G. Khvostantsev, A. G. Lyapin, A. V. Sapelkin and O. B. Tsiok, Nature of semiconductor-to-metal transition and volume properties of bulk tetrahedral amorphous GaSb and GaSb–Ge semiconductors under high pressure, *Phys. Rev. Lett.*, **73**, 3262 (1994).
5. E. G. Ponyatovsky and O. I. Barkalov, Thermobaric quenching – a new method for producing metastable states, *Mater. Sci. Engineering*, **A133**, 726 (1992).
6. E. G. Ponyatovsky and O. I. Barkalov, Pressure-induced amorphous phases, *Mater. Sci. Rep.*, **8**, 147 (1992).
7. V. V. Brazhkin, A. G. Lyapin, S. V. Popova and N. V. Kalyaeva, Preparation of a new class of semiconductors: bulk amorphous tetrahedral solid solutions $Ge_{1-x}(GaSb)_x$, *J. Mater. Sci.*, **30**, 443 (1995).
8. E. Yu. Tonkov, *High Pressure Phase Transformations, A Handbook*, Vols. **1** and **2** [Gordon and Breach, Philadelphia, PA, 1992].
9. M. B. Panish., The pseudobinary system Ge–GaAs, *J. Electrochem. Soc.*, **113**, 626 (1966).
10. K. N. Ishihara, P. H. Shingu, H. Matsueda and Y. Furuhata, Non-equilibrium solid solution formation of (III-V)-IV semiconductors, *Suppl. to Trans. JIM*, **29**, 249 (1988).
11. H. Olijnik, S. K. Sikka and W. B. Holzapfel, Structural phase transitions in Si and Ge under pressures up to 50 GPa, *Phys. Lett.*, **103A**, 137 (1984).
12. T. R. R. McDonald, R. Sard and E. Gregory, Retention of GaSb(II) at low temperatures and one atmosphere pressure, *J. Appl. Phys.*, **36**, 1498 (1965).
13. O. I. Barkalov, E. G. Ponyatovsky and V. E. Antonov, Solid state amorphization of the GaSb high pressure phase, *J. Non-Cryst. Solids*, **156–158**, 544 (1993).
14. V. E. Antonov, O. I. Barkalov and E. G. Ponyatovsky, Crystal-to-amorphous phase transformation of the Ga–Sb high pressure phase, *J. Non-Cryst. Solids*, **192–193**, 443 (1995).
15. V. V. Brazhkin, S. V. Demishev, Yu. V. Kosichkin, D. G. Lunts, A. G. Lyapin, S. V. Popova, N. E. Sluchanko and S. F. Frolov, Anomalies of the structure and electrophysical characteristics of amorphous semiconductor *a*-GaSb:Ge, *Zh. Eksp. Teor. Fiz.*, **104**, 3126 [Engl. Transl. *JETP*, **77**, 465 (1993)] (1993).
16. E. G. Ponyatovsky and T. A. Pozdnyakova, The *T–P* phase diagrams of amorphous GaSb, InSb and InAs, *J. Non-Cryst. Solids*, **188**, 1153 (1995).
17. V. F. Degtyareva and E. G. Ponyatovskii, High-pressure phases in *B* group element alloys: a new sort of electronic phase, *Fiz. Tverd. Tela (Leningrad)*, **24**, 2672 [Engl. Transl. *Sov. Phys. Solid State*, **24**, 1524 (1982)] (1982).
18. O. Mishima, L. D. Calvert and E. Whalley, 'Melting ice' I at 77 K and 10 kbar: a new method of making amorphous solids, *Nature* **310**, 393 (1984).
19. P. Richet, Superheating, melting and vitrification through decompression of high-pressure minerals, *Nature*, **331**, 56 (1988).
20. B. K. Charkraverty, On the excess entropy of fusion of semiconducting and semimetallic elements, *J. Phys. Chem. Solids*, **30**, 454 (1969).
21. A. R. Regel and V. M. Glazov, Structural defects in semiconductors melts, *Fiz. Tekhn. Poluprov.*, **17**, 1729 [Engl. Transl. *Sov. Phys. Semicond.*, **17**, 1105 (1983)] (1983).
22. I. L. Apetkar and E. G. Ponyatovsky, To the theory of the isomorphic phase transformation and the critical transition of cerium, *Dokl. Akad. Nauk SSSR*, **173**, 852 {in Russian} (1967).
23. E. G. Ponyatovskii, V. V. Sinitsyn and T. A. Pozdnyakova, Second critical point and low-temperature anomalies in the physical properties of water, *Pis'ma Zh. Eksp. Teor. Fiz.*, **60**, 352 [Engl. Transl. *JETP Lett.*, **60**, 360 (1994)] (1994).
24. I. L. Aptekar and E. G. Ponyatovskii, Theory of isomorphism of cerium, *Fiz. Metallov i Metallovedinie*, **25**, 777;**25**, 1049 (1968) [Engl. Transl. *Phys. Met Metallogr.*, **25**, 10 (1968); **25**, 93 (1968)] (1968).
25. S. N. Vaidya, Theory of melting, *Phys. Stat. Sol. (a)*, **86**, 565 (1984); **87**, 181 (1985); **91**, 37 (1985).
26. A. Feltz, *Amorphe und Glasartige anorganische Festkörper* [Akademie-Verlag, Berlin, 1983].
27. V. V. Brazhkin, R. N. Voloshin and S. V Popova, Semiconductor-metal transition in Se melt at high pressure, *Pis'ma Zh. Eksp. Teor. Fiz.*, **50**, 392 [Engl. Transl. *JETP Lett.*, **50**, 424 (1989)] (1989).